Laser and Particle Beams (2002), *20*, 243–253. Printed in the USA.

DOI: 10.1017/S0263034602202141

Proton acceleration by fast electrons in laser–solid interactions

J.R. DAVIES
GoLP, Instituto Superior Técnico, 1049-001 Lisboa, Portugal

(Received 16 November 2001; Accepted 22 December 2001)

Abstract

The emission of high-energy protons in laser–solid interactions and the theories that have been used to explain it are briefly reviewed. To these theories we add a further possibility: the acceleration of protons inside the target by the electric field generated by fast electrons. This is considered using a simple one-dimensional model. It is found that for relativistic laser intensities and sufficiently long pulse durations, the proton energy gain is typically several times the fast electron temperature. The results are very similar to those obtained for proton acceleration by electron expansion into vacuum.

Keywords: Fast electrons; Laser–plasma; Laser–solid interactions; Proton acceleration

1. INTRODUCTION

It has long been observed that beams of high-energy protons are emitted when a solid target is irradiated by a laser with an intensity sufficient to create a plasma. Extensive reviews have been given by Gitomer *et al.* (1986) and Mendonça *et al.* (2001). The essential points of interest are that proton emission is observed to be independent of target material, that their energy per charge is greater than that of other ions, that they are generally emitted in a beam normal to the target surface and that their energies are found to be proportional to the fast electron temperature (the electron temperature determined from X-ray emission). In Figure 1, a collection of measured maximum and mean proton energies are plotted against $I\lambda^2$, where I is the intensity and λ is the wave length of the laser. This extends that published by Mendonça *et al.* (2001) to include the subsequent results of Mackinnon *et al.* (2001), Murakami *et al.* (2001), and Roth *et al.* (2001). The region covered by the results collected by Gitomer *et al.* (1986) is outlined with a dotted line. These give the energy associated with the first peak of the ion emission, which should be approximately the mean energy. Both the maximum and mean energies follow the same trend, and can be well fitted by a function of the form $(I\lambda^2)^\alpha$ with α in the range 0.3–0.5. Clark *et al.* (2000*b*) and Mendonça *et al.* (2001) found that the data was best fitted by two separate curves; at low $I\lambda^2$, an α of just over 0.3 gives the best fit, while at high $I\lambda^2$, a value of about 0.5 is indicated. The changeover comes at around 10^{18} W cm^{-2} μm^2. To illustrate the correlation with the fast electron temperature, we plot the result obtained by Beg *et al.* (1996), $kT = 0.215(I\lambda^2)^{1/3}$ eV, where $I\lambda^2$ is in W cm^{-2} μm^2, by fitting experimental results in the range 10^{16}–10^{19} W cm^{-2} μm^2, and the ponderomotive potential, which gives the maximum energy of an electron oscillating in the laser electric field, and better characterizes the fast electron temperature at higher values of $I\lambda^2$. For $I\lambda^2 \gg 10^{18}$ W cm^{-2} μm^2, it scales as $(I\lambda^2)^{1/2}$. This not only illustrates the correlation between proton energy and fast electron temperature, but also illustrates the change in scaling with $I\lambda^2$. Throughout this article, we will consider an example of an intensity of 5×10^{19} W cm^{-2}, a wave length of 1 μm, and a pulse duration of 1 ps, based on the experiments of Clark *et al.* (2000*a*). The maximum proton energy was approximately 30 MeV, the mean energy 2.5 MeV, and the fast electron temperature 2 MeV (Zepf *et al.*, 2001).

The established explanation for these observations is that the protons come from surface contaminants, such as grease, oil, and water, and are accelerated by the electrostatic field set up by fast electrons leaving the target. This immediately explains why the emission is independent of target material, why it is normal to the target surface, and why the proton energies are correlated to the fast electron temperature. Protons gain a higher energy per charge than other ions as they have a higher charge-to-mass ratio, so they are more rapidly

Address correspondence and reprint requests to: J.R. Davies, GoLP, Instituto Superior Técnico, 1049-001 Lisboa, Portugal. E-mail: jdavies@popsrv.ist.utl.pt

accelerated and lower the field seen by other ions. This leaves only the energy gain to be explained. A vast amount of theoretical work has been published on this topic; after all, the problem is essentially that of the expansion of a plasma, a generic problem in plasma physics. This means that we can give only a cursory review of this work; as we are going to develop a one-dimensional (1D) model, we will concentrate on 1D results. For our purposes, it can be briefly summarized as showing that protons can be accelerated to energies greater than the temperature of the electrons that drive the expansion, in agreement with the experimental results. The basic physical reason for this is simply that they have a higher mass, so they can be accelerated to a higher energy without overtaking the electrons.

The simplest model is that of a quasi-neutral fluid with cold protons and inertialess electrons, that is, the electrons are assumed to be always in equilibrium with the electrostatic field, $\mathbf{E} = -\nabla\phi$, and the Boltzmann relation $n \propto \exp(e\phi/kT)$ is used for the electron number density n, which with quasi-neutrality is also the proton number density, or, equivalently, the electric field is assumed to balance the electron pressure gradient $ne\mathbf{E} = -\nabla(nkT)$. This assumes that the electrons have a Maxwellian distribution. The continuity equation and ion equation of motion complete the model. One-dimensional, self-similar solutions for an isothermal expansion have been applied to describe proton acceleration during the laser pulse by various authors (e.g., Crow *et al.*, 1975; Gitomer *et al.*, 1986; Tan *et al.*, 1983; Wilks *et al.*, 2001), the constant temperature and number of particles increasing linearly in time being reasonable approximations while the laser is continually generating fast electrons. In plane geometry, for a uniform plasma situated at $z \leq 0$ at time $t = 0$, the number density at $z > 0$ when $t > 0$ is given by $n = n_0 \exp(-v/c_s)$ where the proton velocity $v = z/t + c_s$ and $c_s = \sqrt{kT/M}$, M being the proton mass. The electric field is given by

$$E = \frac{kT}{ec_s t}, \tag{1}$$

and is constant in space. The proton energy (K) distribution is given by $\exp(-\sqrt{K/kT})$, giving a mean energy of $3kT$ and tending to infinity. Gitomer *et al.* (1986) calculated the energy associated with the peak of the proton current, assuming that their velocities remained constant after the laser pulse, finding it to be approximately $2kT$, independent of the assumed pulse duration. The instantaneous acceleration of the protons to infinity, and infinite energy, is a result of the quasi-neutral approximation. In reality, they would have a finite extent with an electron sheath in front of them and a net positive charge behind. For fixed protons, and no longer assuming quasi-neutrality, the electric field in the electron sheath at $z > 0$ is (Crow *et al.*, 1975)

$$E = \frac{2kT}{e(z + \sqrt{2}\exp(0.5)\lambda_D)}, \tag{2}$$

where λ_D is the electron Debye length in the neutral plasma $(z \to -\infty)$. This gives an upper limit on the electric field of approximately $kT/e\lambda_D$, indicating that Eq. (1) only applies for $c_s t > \lambda_D$. Numerical solution of the non-quasi-neutral problem by Crow *et al.* (1975) showed the expansion of a well defined ion front, appearing as a local peak in the ion density. Their graph of front velocity (v_f) versus time can be approximately fitted by $v_f = 2c_s \ln(1 + c_s t/\lambda_D)$, which gives a good fit for $c_s t \gg \lambda_D$, indicating that the front is then being accelerated by an electric field twice that given by Eq. (1). Behind the front, the electric field falls, tending to the quasi-neutral result given in Eq. (1). The same maximum ion velocity for $c_s t \gg \lambda_D$ can be obtained by applying the condition $c_s t \geq \lambda_D(z)$ to the quasi-neutral solution, where $\lambda_D(z)$ is the electron Debye length at position z (Tan *et al.*, 1983); this gives a maximum z and hence a maximum v. The maximum ion energy still tends to infinity as time tends to infinity. Tan *et al.* (1983) assumed that the proton velocities remained fixed after the pulse to give a finite maximum energy. For the range of parameters covered by the experimental results collected in Figure 1, this gives maximum energies in the range of roughly (1–200)kT, the higher values being obtained for the lower intensity experiments using nanosecond pulses. The experimental results fall in the range of roughly (5–30)kT. Clearly this model is inadequate, and there is no physical reason for assuming that the proton velocities remain fixed after the pulse. Whatever fluid model is used, infinite maximum energies will always be obtained, as the Maxwellian electron distribution assumed extends to infinity. There is no inherent contradiction in the model because it gives infinite energies. In reality there would be a maximum energy, if for no other reason than that we are dealing with particles of finite mass and not a fluid. We expect the maximum ion energy to be determined by the maximum electron energy, which in turn will be determined by the laser–plasma interaction, which is beyond the scope of our considerations.

Analytic solutions to other quasi-neutral, cold-ion models have also been found, for example, Wickens *et al.* (1978) considered a two-temperature electron distribution and, for a more recent example, Dorozhkina and Semenov (1998) considered the adiabatic expansion of a plasma using the Vlasov equation for the electrons. As we are considering ion acceleration by a small, high-temperature fraction of the target electrons (the fast electrons) a two-temperature model is of particular interest. Wickens *et al.* (1978) found that if the temperatures differ by a factor of 10 or more, decoupling occurs, and the quasi-neutral solution breaks down. This justifies considering the fast electrons independently. Other fluid models have also been used, some of them considerably more complex, requiring numerical solution. Gitomer *et al.* (1986) considered a variety of such models of increasing complexity. This is one of the few treatments that actually considers a layer of hydrogen on a heavier target element; most models consider a hydrogen plasma. They found that if the absorption into fast electrons was sufficient, the fast

https://doi.org/10.1017/S0263034602202141 Published online by Cambridge University Press

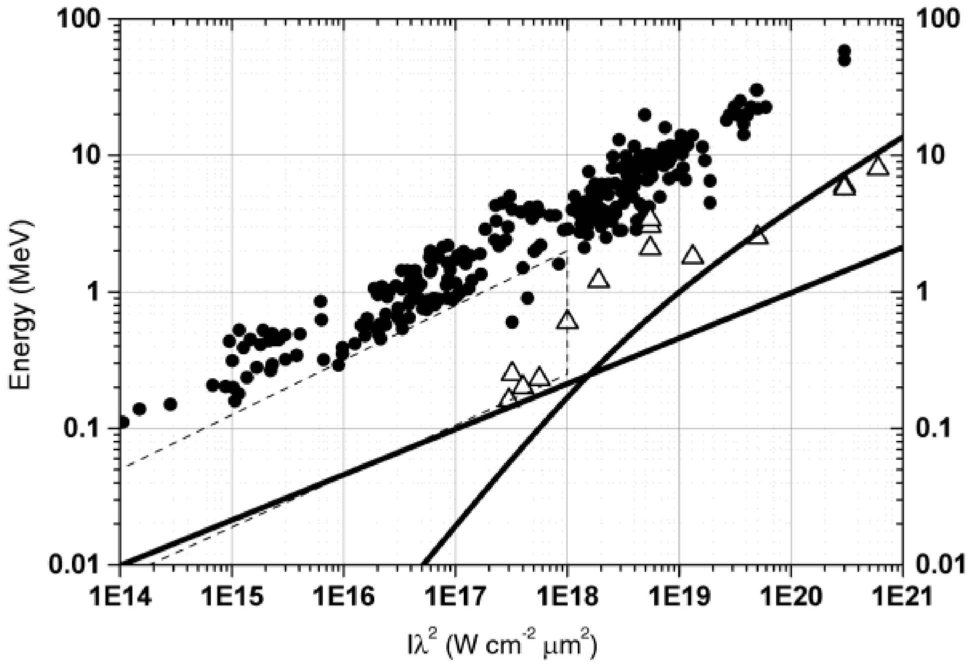

Fig. 1. Measured maximum proton energies (dots) and mean proton energies (triangles) as a function of $I\lambda^2$. The dotted line indicates the region of the data collected by Gitomer *et al.* (1986). The straight line is the fast electron temperature given by Beg *et al.* (1996). The curve is the ponderomotive potential.

electrons and the protons decoupled from the rest of the target, an essential assumption in applying the simpler models. The problem has also been studied with PIC codes, for example, by Murakami *et al.* (2001), Pukhov (2001), and Wilks *et al.* (2001). The problem would thus appear to have been largely resolved. However, the more recent results included in Figure 1, which are at the higher values of $I\lambda^2$, are for proton emission from the rear of targets (opposite surface to that irradiated by the laser), whereas the others are for emission from the front. Ion emission from the rear of targets has been reported before, for example, by Ebrahim *et al.* (1979), Marjoribanks *et al.* (1980), and Tsakiris *et al.* (1981). What has renewed interest in it is that, even for relatively thick targets, the highest energy protons are emitted from the rear, and in a narrower cone angle. Emission from the rear could not only come from impurities accelerated off the rear surface, but also from protons moving through or around the target. Protons accelerated through the target could not only come from surface impurities but also from within the target; even metals can contain significant quantities of hydrogen, trapped in the lattice. Clark *et al.* (2000*a*), Krushelnick *et al.* (2000), Maksimchuk *et al.* (2000), Nemoto *et al.* (2001), and Zepf *et al.* (2001) attribute their measurements to protons originating from an extended region at the front of the target. However, for very similar experiments, Hatchett *et al.* (2000), Snavely *et al.* (2000), MacKinnon *et al.* (2001), Murakami *et al.* (2001), and Roth *et al.* (2001) attribute their measurements to protons originating from the rear surface, and something of a controversy has arisen. There are thus more mechanisms than that discussed above that need to be evaluated. Transport around the target was used by Ebrahim *et al.* (1979) and Marjoribanks *et al.* (1980) to explain their results, and is also reported by Krushelnick *et al.* (2000). However, this is clearly not the source of protons with a higher energy than those measured at the front, nor of the narrow beams observed (Tatarakis *et al.*, 1998). Acceleration of protons into targets has been seen in PIC code modeling of laser interaction with overdense plasma (e.g., Wilks, 1993; Wilks *et al.*, 1992, 2001; Pukhov, 2001); the charge separation set up by the ponderomotive force accelerates protons to energies of the order of the ponderomotive potential. A further possibility is that protons are accelerated by the electric field generated by fast electrons inside the solid target. This generation of electric field by fast electrons has been considered by a number of authors. We will consider the work of Bell *et al.* (1997), who obtained analytic solutions to a 1D model very similar to those discussed above. This provides an excellent starting point for a consideration of proton acceleration in solid targets, paralleling that on acceleration into vacuum.

2. THE MODEL

The basic equations used by Bell *et al.* (1997) are the same as those of the quasi-neutral fluid model discussed above, except instead of assuming that the electrons are neutralized by a flow of ions, it is assumed that they are neutralized by a return current of electrons from the solid target, referred to as the background. This is represented by Ohm's law $E = \eta j_b$, which is used in place of the ion equation of motion, where η is resistivity, assumed to be constant, and j_b is background current density. Neutrality requires current balance, giving, in 1D $j_b = -j_f$, where j_f is the fast electron current density. This gives an electric field that opposes the fast electron propagation into the target, and that would accelerate protons into the target. Assuming that the number density of protons is much less than that of the fast electrons, the proton energy gain can be calculated by integrating this electric field. As the total number of protons measured from the rear of targets is typically much less than the expected number of fast electrons, this appears to be a reasonable assumption. The model also assumes that the background electrons respond instantaneously, and that the fast electron density is much less than that of the background electrons. From the continuity equation of the background electrons, it can be shown that their response time is given by $\varepsilon_0\eta$, so all time scales must be much greater than this. At most it is of the order of 10^{-17} s, much lower than typical laser periods. The electron plasma period at solid density (10^{29}–10^{30} electrons m^{-3}) is also of this order, so for low resistivities, it would set the minimum time scale. This also sets a minimum spatial scale of the speed of light times the minimum time scale. Bell *et al.* (1997) found an isothermal solution with the number of fast electrons growing linearly in time and a solution with a constant number of fast electrons and a temperature that varies in time, but not space. The first of these is intended to describe the transport during the laser pulse and the latter after the laser pulse. The electric field during the pulse is given by

$$E = \frac{2kT}{e(z + L_0)}, \tag{3}$$

where L_0 is the distance over which the number density halves. It is determined by setting the absorbed laser energy equal to the fast electron kinetic energy; the electrostatic energy is negligible in comparison for $t \gg \varepsilon_0\eta$. Bell *et al.* (1997) used a mean fast electron energy of $3kT/2$, the non-relativistic result for a Maxwellian distribution with three velocity components, or in other words, 3 degrees of freedom. We use the non-relativistic, 1D result, $kT/2$, giving

$$L_0 = \frac{(kT)^2}{e^2\eta I_{abs}}, \tag{4}$$

a factor of 3 lower, where I_{abs} is the laser intensity absorbed into fast electrons (in W m^{-2}). In the relativistic case, the energy per degree of freedom increases with temperature from $kT/2$ for $kT \ll mc^2$ to kT for $kT \gg mc^2$. Our choice gives an upper limit on the electric field and hence on the proton acceleration. Equation (3) is the same as Eq. (2) with L_0 in place of $\sqrt{2}\exp(0.5)\lambda_D$. As Eq. (2) gives an upper limit on the electric field, we must have $L_0 \gg \lambda_D$; again this requires $t \gg \varepsilon_0\eta$. For our example, we will consider an absorption into fast electrons of 30% and a resistivity of 2×10^{-6} Ω m, a typical upper limit (Milchberg *et al.*, 1988; Davies *et al.*, 1999), giving $L_0 = 13.3$ μm and a maximum electric field $2kT/eL_0 = 3 \times 10^{11}$ V m^{-1}. The electric field after the pulse is given by

$$E = \frac{2kTz}{e(z^2 + L_t^2)}, \tag{5}$$

where the distance over which the number density halves, L_t, now depends on time. It is determined by the time dependence of the temperature and the requirement that $L_t = L_0$ at the end of the pulse. Bell *et al.* (1997) assumed an adiabatic expansion, which for our choice of mean energy gives a temperature $T(L_0/L_t)^2$ and

$$L_t = L_0\left(\frac{3\pi}{2\tau}(t - \tau) + 1\right)^{1/3}, \tag{6}$$

where τ is the laser pulse duration. For a mean energy αkT, temperature falls as $(L_0/L_t)^{1/\alpha}$ and in Eq. (6) the 3s are replaced by $1 + 1/\alpha$. Our choice again gives an upper limit on the field. Note that this result does not apply in the relativistic case. These solutions for the electric field are plotted in Figure 2. The energy gain (ΔK) during the pulse is thus

$$\Delta K = 2kT \ln\frac{z + L_0}{z_0 + L_0}, \tag{7}$$

where z_0 is the initial position. We cannot solve for the energy gain as an explicit function of time, but it is clear that the time dependence will be logarithmic and that the energy gain will increase more rapidly for higher initial energies. As mentioned in the introduction, PIC modeling shows that protons are accelerated into the target with energies of the order of the ponderomotive potential, which for $I\lambda^2 > 10^{18}$ W cm^{-2} μm^2 is approximately the fast electron temperature, so we will consider protons with nonzero initial energies. The electric field after the pulse cannot be integrated analytically, but, from analyzing the form of the electric fields shown in Figure 2, it is clear that the above expression is a good approximation for the maximum energy gain. To achieve this maximum energy gain, a proton must have $z \geq L_0$ at the end of the pulse, and must not be overtaken by the peak in the electric field at $z = L_t$, which has a velocity

$$\frac{dL_t}{dt} = \frac{\pi}{2}\frac{L_0}{\tau}\left(\frac{L_0}{L_t}\right)^2. \tag{8}$$

Maximum energy gain is guaranteed for an initial velocity $v_0 > L_0/\tau$, for $z_0 \gg L_0$ and for a long enough pulse duration. For protons starting at the target surface $z_0 = 0$, the condition $z > L_0$ at the end of the pulse is sufficient for Eq. (7) to be a good approximation for the total energy gain. The minimum pulse duration this requires as a function of initial energy is given in Figure 3. The essential time scale of proton acceleration (t_0) is $L_0/\sqrt{2kT/M}$, or

https://doi.org/10.1017/S0263034602202141 Published online by Cambridge University Press

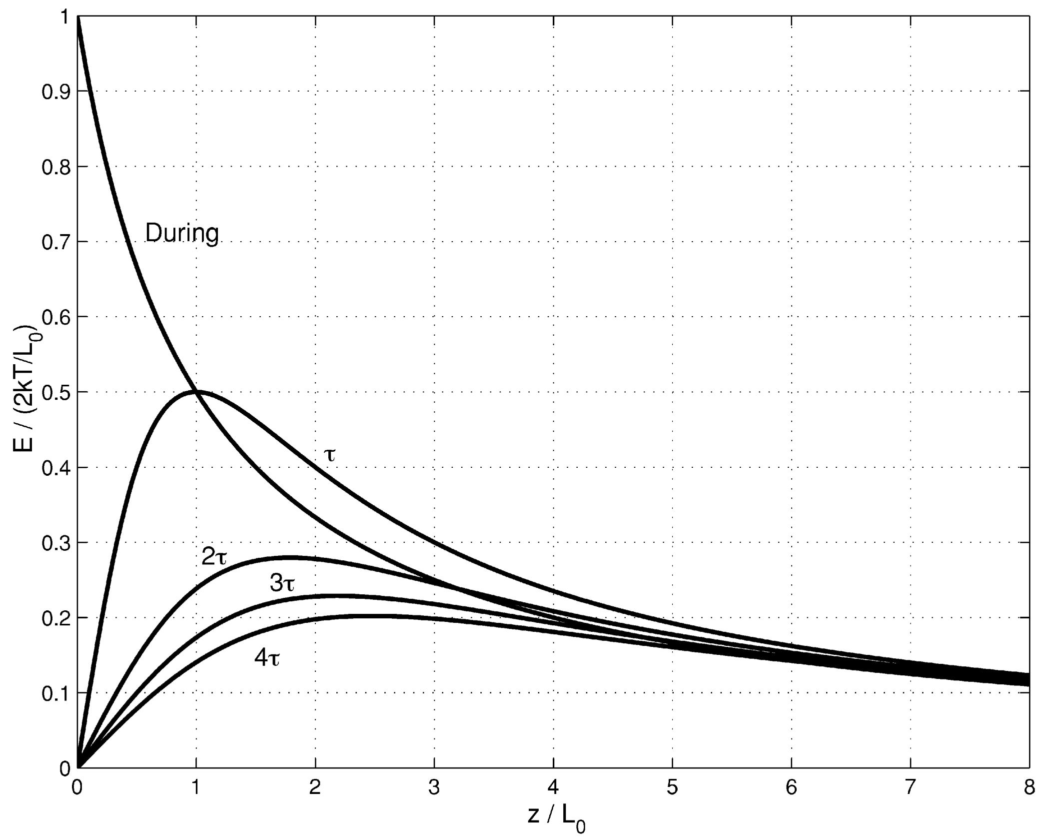

Fig. 2. The electric field during the pulse and at various times after the pulse; τ is the pulse duration.

$$t_0 = \sqrt{\frac{M}{2}}\,\frac{(kT)^{3/2}}{e^2\eta I_{abs}}, \tag{9}$$

which is 0.668 ps for our example. For higher values of z_0 the required pulse duration is lower, so for pulse durations $\tau > 1.52t_0$, Eq. (7) will apply to all protons, which is the case for our example. For an initial energy of kT, the minimum pulse duration is $0.77t_0$. For greater pulse durations, the proton acceleration does not vary, while for lower values, it falls off rapidly. This is illustrated in Figures 4 and 5, which give the energy gain as a function of time and position, respectively, for protons with $z_0 = 0$ and initial energies of 0 and kT and various pulse durations. The energy gain can slightly exceed the value given by Eq. (7), as would be expected from the electric fields shown in Figure 2. Figure 4 clearly illustrates the far more rapid acceleration of protons that are already in motion. It can be shown that for energy gains much greater than both $2kT$ and the initial energy, the difference in energy gain between protons with differing initial energies is just the difference in the initial energies.

This model, like those for acceleration into vacuum, gives no limit on the maximum energy gain, though it requires infinite time and distance to achieve infinite energies. There are a number of effects that could limit the energy gain, such as finite target thickness, a maximum fast electron energy, energy loss of the fast electrons to the protons, stopping of the fast electrons by collisions, and stopping of the protons by collisions. The target thickness in Eq. (7) gives an absolute upper limit on the energy gain in the target. A maximum electron energy would limit the energy gain to this value, as once the highest energy electron has been turned around by the electric field, there will be no fast electron current, and, hence, in this model, no electric field. We expect the electron energy loss to the protons to be unimportant. For protons and electrons of the same energy, travelling faster than the mean speed of the background electrons, the collisional energy loss to the background electrons is $M/m = 1836$ times greater for the protons than the fast electrons, so in general, collisional losses will be greater for the protons than for the fast electrons, so we will consider this in more detail. For purposes of comparison, we define a collisional electric field E_c, such that eE_c gives the deceleration due to collisions. Taking the result given by Spitzer (1962), we see that it depends on the ratio of the proton energy to the background electron temperature kT_b, reaching a maximum when the proton energy is 1836 times higher. Typically this will be lower than the energies we are interested in, so we will only consider this maximum value and the high energy limit. The maximum value is

$$(E_c)_{max} \approx 0.21\,\frac{eD}{kT_b}, \tag{10}$$

https://doi.org/10.1017/S0263034602202141 Published online by Cambridge University Press

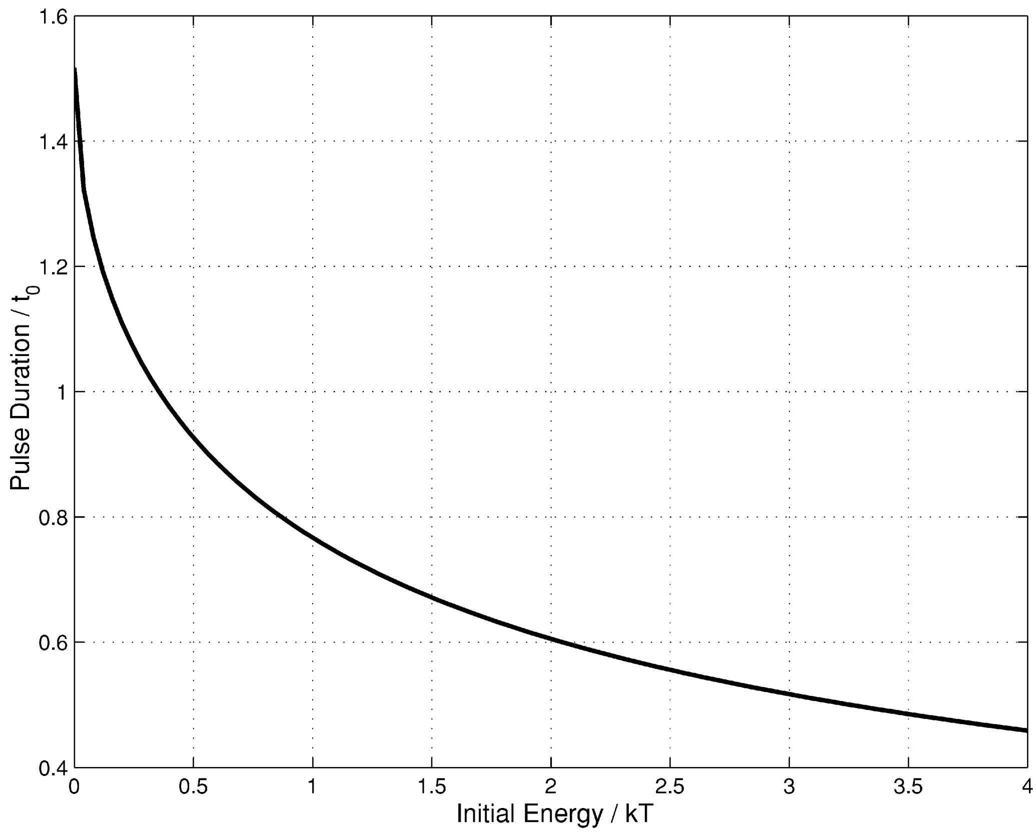

Fig. 3. The minimum pulse duration required to obtain maximum energy gain as a function of initial proton energy for a proton starting at $z_0 = 0$.

where $D = n_b e^2 \ln\Lambda/4\pi\varepsilon_0^2$, where n_b is the background electron density and $\ln\Lambda$ is a weakly varying function of proton energy and background material, typically of order 10. The atom number density of solids does not vary significantly, and is typically $6 \times 10^{28}\ \mathrm{m}^{-3}$, putting $n_b = 6 \times 10^{28} Z\,\mathrm{m}^{-3}$ and kT_b in electron volts gives $3.28 \times 10^{11} Z \ln\Lambda/kT_b\ \mathrm{V\,m}^{-1}$. For protons to be accelerated to energies greater than $1836kT_b$, the maximum electric field $2kT/eL_0$ must be greater than $(E_c)_{max}$, which requires

$$I_{abs} > 0.105\,\frac{D}{\eta}\,\frac{T}{T_b}, \tag{11}$$

where I_{abs} is in $\mathrm{W\,m}^{-2}$. Considering our example parameters and an aluminum target with $Z = 13$, $\ln\Lambda = 10$, and $kT_b = 50$ eV, the temperature at which the resistivity peaks (Milchberg *et al.* 1988), gives $4.3 \times 10^{19}\ \mathrm{W\,cm}^{-2}$, greater than the actual value of $1.5 \times 10^{19}\ \mathrm{W\,cm}^{-2}$. To give a minimum absorbed intensity of this value would require $kT_b > 142$ eV, but at this temperature, the resistivity is lower and falls faster than $1/T_b$. Taking account of the fact that, in general, the resistivity falls at high temperatures and that the temperature will increase with absorbed intensity greatly complicates the situation. It appears to be finely balanced as to whether an electric field greater than $(E_c)_{max}$ could be generated. Thus collisions will tend to limit the acceleration of low energy protons to energies less than $1836kT_b$. This indicates that the initial proton acceleration must occur in lower density, higher temperature plasma, such acceleration has been predicted by PIC codes, as mentioned in the introduction. For proton energies $K \gg 1836kT_b$

$$E_c \approx \frac{1}{2}\,\frac{M}{m}\,\frac{eD}{K}, \tag{12}$$

which is within 10% of the actual value for $K > 5700kT_b$. Requiring the maximum electric field to exceed this gives

$$I_{abs} > 460\,\frac{D}{\eta}\,\frac{kT}{K}. \tag{13}$$

For our example, this is $4.7 \times 10^{18} kT/K\ \mathrm{W\,cm}^{-2}$, requiring $K > 0.31kT$. As for $I\lambda^2 > 10^{18}\ \mathrm{W\,cm}^{-2}\ \mu\mathrm{m}^2$ proton energies entering the target of the order of kT are expected, this condition should be fulfilled. To illustrate the combined effect of the electric field and the collisional drag, given by Eq. (12), we give proton energy as a function of position for our example case and various initial energies in Figure 6. This shows a maximum energy gain that increases with

https://doi.org/10.1017/S0263034602202141 Published online by Cambridge University Press

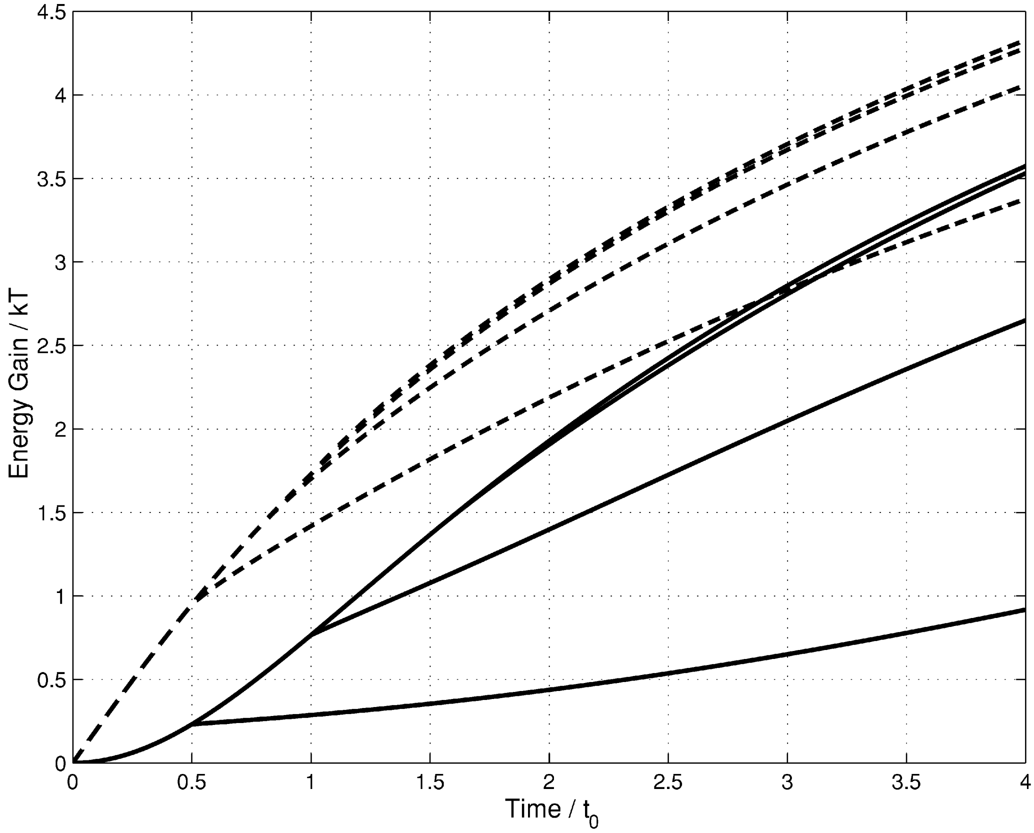

Fig. 4. Proton energy gain as a function of time for protons with zero initial energy (solid line) and an initial energy of kT (dashed line) starting at $z_0 = 0$. Pulse durations of $0.5t_0$, t_0, $4t_0$, and that given in Figure 3 are shown.

initial energy, very rapidly so that the threshold energy of $0.31kT$ is exceeded. For an initial energy of $0.36kT$ (0.72 MeV), the maximum energy gain is only $0.048kT$ (0.095 MeV), while for an initial energy of $0.5kT$ (1 MeV) it increases considerably to $1.22kT$ (2.43 MeV), and for an initial energy of kT (2 MeV), it is $2.85kT$ (5.69 MeV). The proton energy eventually falls with distance, so there would be an optimum target thickness to maximize the energy gain in the target.

3. CONCLUSIONS

The electric field generated by fast electrons in solid targets can accelerate protons through the target, with typical energy gains of the order of the fast electron temperature. The energy gain increases with the initial energy of the proton. For optimum energy gain, protons must be accelerated into the target with the fast electrons, as has been predicted by PIC codes. Simple estimates indicate that proton acceleration inside the target requires $I\lambda^2 > 10^{18}$ W cm^{-2} μm^2 and pulse durations greater than roughly t_0, given in Eq. (9).

Proton energy gain in the target is limited by collisional energy loss of the protons to the target electrons, but protons will continue to be accelerated by the fast electrons on leaving the target. The results for the typical energy gain by acceleration into vacuum, from comparable models, are basically the same, for the same fast electron parameters. Both models are in general agreement with the experimental measurements of mean energies presented in Figure 1. The maximum energy gain is not determined by the simple fluid models; we expect it to be determined by the maximum fast electron energy.

If the electric field generated by the fast electrons inside the target is sufficient to give significant proton energy gain, then that at the rear surface will be lower. However, it should be taken into account that protons accelerated through the target could gain more energy at the rear surface than those accelerated from rest, like a multistage accelerator. The acceleration of protons from the laser interaction region, through the target, and out to the detectors is, of course, a continuous process; it is just that we have to make different approximations in different regions to produce tractable models. This means that the relative importance of acceleration inside and out of the target and the origin of the protons could not be readily determined from measurements of the proton energy. The essential differences between the two acceleration processes are that the number density of protons that can be accelerated in the target is much lower than that of the fast electrons, while outside it is equal, and that inside the target, collisions prevent the acceleration of low

https://doi.org/10.1017/S0263034602202141 Published online by Cambridge University Press

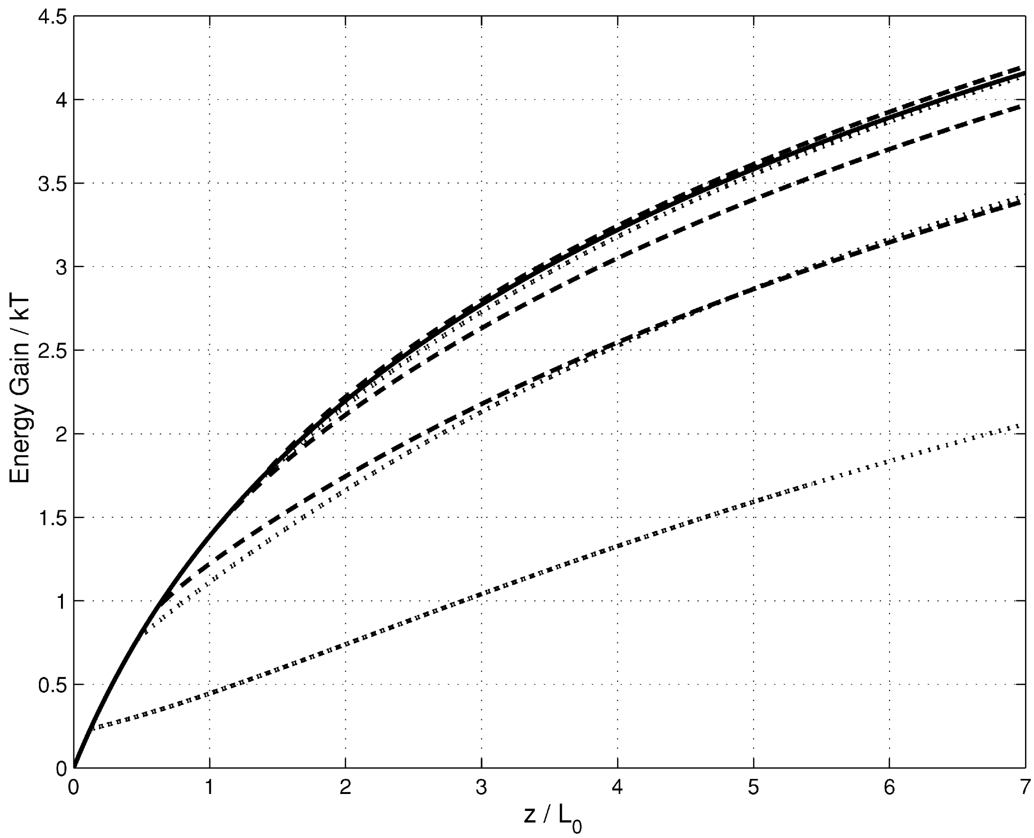

Fig. 5. Proton energy gain as a function of depth for protons with zero initial energy (dotted line) and an initial energy of kT (dashed line) starting at $z_0 = 0$. Pulse durations of $0.5t_0$, t_0, $4t_0$, and that given in Figure 3 are shown. The solid line is the analytic result during the pulse $2kT\ln(1 + z/L_0)$.

energy protons and heavier ions, while outside all ions will be accelerated. If acceleration inside the target is the main contributor to the ion emission from the rear, then there should be relatively few heavy ions, with a much lower energy per charge. As the fast electron number density at the rear surface would then be much lower than that inside the target, the number of protons accelerated off the rear surface would not necessarily be greater than that inside the target. Clark *et al.* (2000*a*, 2000*b*) report measurements of ion emission at the front and rear of targets from the same series of experiments. The relative number and energy per charge of heavy ions emitted from the front was significantly greater than that from the rear, consistent with a significant contribution from acceleration through the target, though not conclusive.

The relative importance of the two processes will change with target thickness, but given that the energy gains are similar, we would just expect the proton energies to start falling beyond a certain thickness due to collisional energy loss in the target. However, the nature of the field generation inside the target and the laser interaction, which determines the fast electron parameters, vary with target thickness. In other words, what happens in a 1-μm-thick target is not necessarily what is happening in the first 1 μm of a 10-μm-thick target. Thus the interpretation of experiments using a series of target thicknesses, such as those of Maksimchuk *et al.* (2000) and Murakami *et al.* (2001), is not as straightforward as it might seem. The field generation, and hence the target conditions, vary because electrons are reflected by the sheath electric field generated at the rear surface. According to our model, this effect should be significant for thicknesses less than the order of L_0 (the model assumed a semi-infinite target, so is only a good approximation for thicknesses much greater than L_0). The laser interaction can be more directly affected in targets thinner than $c\tau/2$ as electrons reflected at the rear surface can re-interact with the laser. Laser interaction with targets with thicknesses comparable to the laser wavelength is known to be quite different from that with thicker targets, as discussed by Mendonça *et al.* (2001). The fact that the rear surface affects the field generation inside the target and that protons accelerated through the target are also accelerated out of the target means that varying the shape of the rear surface, reported by Hatchett *et al.* (2000), Krushelnick *et al.* (2000), Snavely *et al.* (2000), and Zepf *et al.* (2001), also does not give a clear indication of the origin of the proton emission. Clearly this is beyond a 1D model. On the basis of these 1D, quasi-neutral fluid models we cannot readily distinguish between

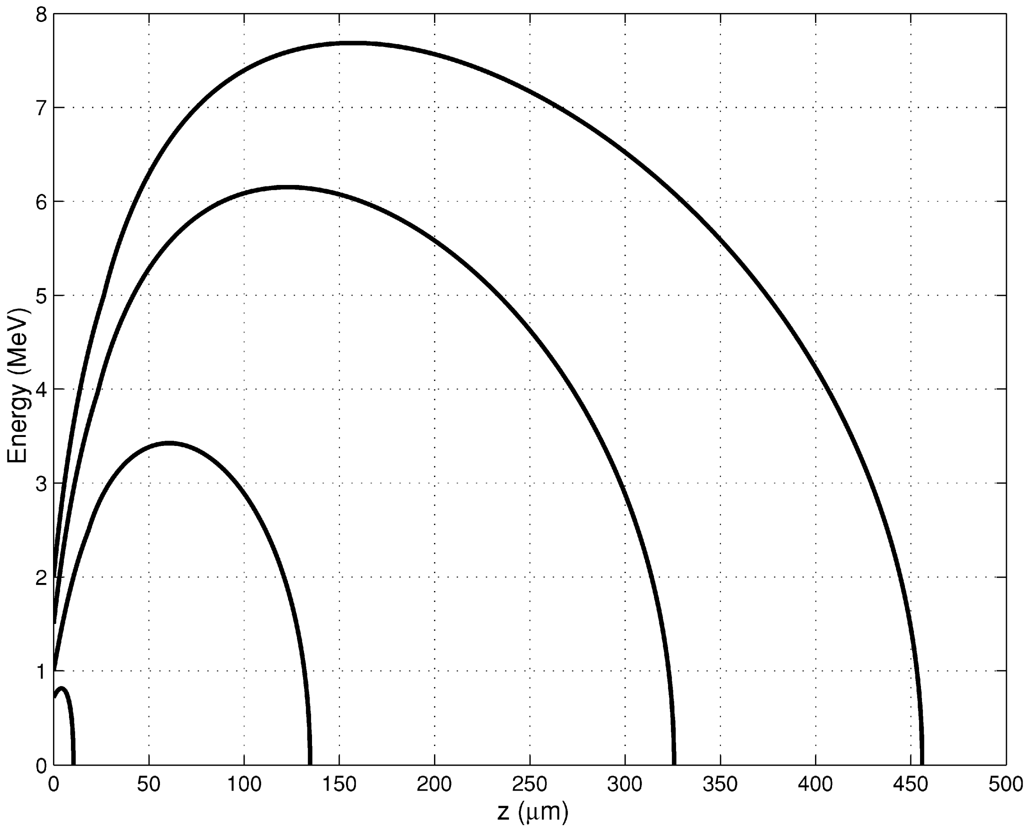

Fig. 6. Proton energy as a function of depth for the example parameters discussed in the text, including collisional energy loss.

acceleration inside and out of the target; thus it is difficult to compare our results with experiments.

The model is of limited validity, being 1D and assuming a fixed resistivity. In general, we expect it to give an upper limit on the proton acceleration. We used an upper limit on the resistivity, so including the variation in resistivity with temperature would only lower the electric field. Electric field generation implies rapid heating of the target to high temperatures, so we expect a rapid fall in the resistivity and hence in the electric field. This represents the main limit on the field generation, and thus on proton acceleration. In three dimensions, we would expect a lower fast electron current density and hence a lower electric field. However, in more than one dimension, the finite transverse extent of the fast electron beam will lead to a growing magnetic field from $\partial \mathbf{B}/\partial t = -\nabla \times \mathbf{E}$. Current balance no longer requires the currents to be coincident. This acts to deflect the electrons into the region of higher electric field, increasing the field generation. This is the only effect that could increase the electric field from the 1D limit, but the magnetic field deflects the protons in the opposite direction to the fast electrons, that is, away from the electric field, so acceleration is not necessarily increased. The deflection decreases with increasing proton energy, so this would lead to a further dependence of energy gain on initial energy. Protons would leave the target at an increasing distance and angle to the electron beam the lower their energy. Such an emission pattern has been reported in experiments by Clark *et al.* (2000*a*), Krushelnick *et al.* (2000), Murakami *et al.* (2001), and Zepf *et al.* (2001). Clark *et al.* (2000*a*) used it to calculate the magnetic field inside the target, but only took into account the collisional energy loss of the protons. Acceleration of protons by the electric field, implied by the very presence of the magnetic field, would lower the magnetic field obtained. However, magnetic field is also generated by emission from the target. This has been considered by a number of authors, such as Craxton and Haines (1978), Murakami *et al.* (2001), and Pukhov (2001). These results do not show proton emission at specific angles that increase with decreasing energy and do not give a sufficient magnetic field to account for the observed proton angles. Thus this emission could be indicative of acceleration in the target. Separation of the lower energy protons from the fast electrons by the magnetic field inside the target gives a possible means of distinguishing between acceleration inside and out of the target. This emission was observed to have a sharp low energy cutoff, as expected for protons that had travelled through the target. However, to clearly distinguish between protons accelerated through the target and those accelerated off the rear surface, it would be necessary to use targets that only contain protons in specific locations. Even then one would have to account for the fact that the presence of

https://doi.org/10.1017/S0263034602202141 Published online by Cambridge University Press

protons at the front of the target will change the laser interaction conditions, as the laser will effectively be interacting with a hydrogen plasma.

The model presented here represents a first, basic step in considering the acceleration of protons by fast electrons inside solid targets. The next step would be to move to more detailed 2D models, such as that described by Davies *et al.* (1997, 1999), possibly including the protons in a self-consistent manner.

REFERENCES

Beg, F.N., Bell, A.R., Dangor, A.E., Danson, C.N., Fews, A.P., Glinsky, M.E., Hammel, B.A., Lee, P., Norreys, P.A. & Tatarakis, M. (1996). A study of picosecond laser-solid interactions up to 10^{19} W cm^{-2}. *Phys. Plasmas* **4**, 447–457.

Bell, A.R., Davies, J.R., Guerin, S. & Ruhl, H. (1997). Fast electron transport in high-intensity short-pulse laser–solid experiments. *Plasma Phys. Control. Fusion* **39**, 653–659.

Clark, E.L., Krushelnick, K., Davies, J.R., Zepf, M., Tatarakis, M., Beg, F.N., Machacek, A., Norreys, P.A., Santala, M.I.K., Watts, I. & Dangor, A.E. (2000*a*). Measurements of energetic proton transport through magnetised plasma from intense laser interaction with solids. *Phys. Rev. Lett.* **84**, 670–673.

Clark, E.L., Krushelnick, K., Zepf, M., Tatarakis M., Machacek, A., Santala, M.I.K., Watts, I., Norreys, P.A. & Dangor, A.E. (2000*b*). Energetic heavy-ion and proton generation from ultraintense laser–plasma interactions with solids. *Phys. Rev. Lett.* **85**, 1654–1657.

Craxton, R.S. & Haines, M.G. (1978). $\mathbf{J} \times \mathbf{B}$ acceleration of fast ions in laser–target interactions. *Plasma Phys.* **20**, 487–502.

Crow, J.E., Auer, P.L. & Allen, J.E. (1975). The expansion of a plasma into a vacuum. *J. Plasma Phys.* **14**, 65–76.

Davies, J.R., Bell, A.R., Haines, M.G. & Guerin, S.M. (1997). Short-pulse high-intensity laser-generated fast electron transport into thick solid targets. *Phys. Rev. E* **56**, 7193–7203.

Davies, J.R., Bell, A.R. & Tatarakis, M. (1999). Magnetic focusing and trapping of high-intensity laser-generated fast electrons at the rear of solid targets. *Phys. Rev. E* **59**, 6032–6036.

Dorozhkina, D.S. & Semenov, V.E. (1998). Exact solution of the problem of quasineutral expansion into vacuum of a localized collisionless plasma with cold ions. *JETP Lett.* **67**, 573–578.

Ebrahim, N.A., Joshi, C., Villeneuve, D.M., Burnett, N.H. & Richardson, M.C. (1979). Anomalous energy transport to rear surface of microdisks at high laser irradiances. *Phys. Rev. Lett.* **43**, 1995–1998.

Gitomer, S.J., Jones, R.D., Begay, F., Ehler, A.W., Kephart, J.F. & Kristal, R. (1986). Fast ions and hot electrons in the laser–plasma interaction. *Phys. Fluids* **29**, 2679–2688.

Hatchett, S.P., Brown, C.G., Cowan, T.E., Henry, E.A., Johnson, J.S., Key, M.H., Koch, J.A., Langdon, A.B., Lasinski, B.F., Lee, R.W., MacKinnon, A., Pennington, D.M., Perry, M.D., Phillips, T.W., Roth, M., Sangster, T.C., Singh, M.S., Snavely, R.A., Stoyer, M.A., Wilks, S.C. & Yasuike, K. (2000). Electron, photon, and ion beams from the relativistic interaction of petawatt laser pulses with solid targets. *Phys. Plasmas* **7**, 2076–2082.

Krushelnick, K., Clark, E.L., Zepf, M., Davies, J.R., Beg, F.N., Machacek, A., Santala, M.I.K., Tatarakis, M., Watts, I., Norreys, P.A. & Dangor, A.E. (2000). Energetic proton production from relativistic laser interaction with high density plasmas. *Phys. Plasmas* **7**, 2055–2061.

MacKinnon, A.J., Borghesi, M., Hatchett, S., Key, M.H., Patel, P.K., Campbell, H., Schiavi, A., Snavely, R., Wilks, S.C. & Willi, O. (2001). Effect of plasma scale length on multi-MeV proton production by intense laser pulses. *Phys. Rev. Lett.* **86**, 1769–1772.

Maksimchuk, A., Gu, S., Flippo, K., Umstadter, D. & Bychenkov, V. Yu. (2000). Forward ion acceleration in thin films driven by a high-intensity laser. *Phys. Rev. Lett.* **84**, 4108–4111.

Marjoribanks, R.S., Burgess, M.D.J., Enright, G.D. & Richardson, M.C. (1980). Propagation of the superthermal corona from CO_2-laser-irradiated microtargets. *Phys. Rev. Lett.* **45**, 1798–1801.

Mendonça, J.T., Davies, J.R. & Eloy, M. (2001). Proton and neutron sources using terawatt lasers. *Meas. Sci. Technol.* **12**, 1801–1812.

Milchberg, H.M., Freeman, R.R., Davey, S.C. & More, R.M. (1988). Resistivity of a simple metal from room temperature to 10^6 K. *Phys. Rev. Lett.* **61**, 2364–2367.

Murakami, Y., Kitagawa, Y., Sentoku, Y., Mori, M., Kodama, R., Tanaka, K.A., Mima, K. & Yamanaka, T. (2001). Observation of proton rear emission and possible gigagauss scale magnetic fields from ultra-intense laser illuminated plastic target. *Phys. Plasmas* **8**, 4138–4143.

Nemoto, K., Maksimchuk, A., Banerjee, S., Flippo, K., Mourou, G., Umstadter, D. & Bychenkov, V. Yu. (2001). Laser-triggered ion acceleration and table top isotope production. *Appl. Phys. Lett.* **78**, 595–597.

Pukhov, A. (2001). Three-dimensional simulations of ion acceleration from a foil irradiated by a short-pulse laser. *Phys. Rev. Lett.* **86**, 3562–3565.

Roth, M., Cowan, T.E., Brown, C., Christl, M., Fountain, W., Hatchett, S., Johnson, J., Key, M.H., Pennington D.M., Perry, M.D., Phillips, T.W., Sangster, T.C., Singh, M., Snavely, R., Stoyer, M., Takahashi, Y., Wilks, S.C. & Yasuike, K. (2001). Intense ion beams accelerated by petawatt-class lasers. *Nucl. Instrum. Methods Phys. Res. A* **464**, 201–205.

Snavely, R.A., Key, M.H., Hatchett, S.P., Cowan. T.E., Roth, M., Phillips, T.W., Stoyer, M.A., Henry, E.A., Sangster, T.C., Singh, M.S., Wilks, S.C., MacKinnon, A., Offenberger, A., Pennington, D.M., Yasuike, K., Langdon, A.B., Lasinski, B.F., Johnson, J., Perry. M.D. & Campbell, E.M. (2000). Intense high-energy proton beams from petawatt-laser irradiation of solids. *Phys. Rev. Lett.* **85**, 2945–2948.

Spitzer, L. (1962). *Physics of Fully Ionized Gases*. New York: Wiley.

Tatarakis, M., Davies, J.R., Lee, P., Norreys, P.A., Kassapakis, N.G. Beg, F.N., Bell, A.R., Haines, M.G. & Dangor, A.E. (1998). Plasma formation on the front and rear of plastic targets due to high-intensity laser-generated fast electrons. *Phys. Rev. Lett.* **81**, 999–1002.

Tan, T.H., McCall, G.H. & Williams, A.H. (1983). Determination of laser intensity and hot-electron temperature from fastest ion velocity measurements. *Phys. Fluids* **27**, 296–301.

Tsakiris, G.D., Eidmann, K., Petsch, R. & Sigel, R. (1981). Experimental studies of the bilateral ion blowoff from laser-irradiated thin plastic folis. *Phys. Rev. Lett.* **46**, 1202–1206.

Wickens, L.M., Allen, J.E. & Rumsby, P.T. (1978). Ion emission from laser-produced plasmas with two electron temperatures. *Phys. Rev. Lett.* **41**, 243–246.

Wilks, S.C. (1993). Simulations of laser-plasma interactions. *Phys. Fluids* **5**, 2603–2608.

Wilks, S.C., Kruer, W.L., Tabak, M. & Langdon, A.B. (1992). Absorption of ultra-intense laser pulses. *Phys. Rev. Lett.* **69**, 1383–1386.

Wilks, S.C., Langdon, A.B., Cowan, T.E., Roth, M., Singh, M., Hatchett, S., Key, M.H., Pennington, D., MacKinnon, A. & Snavely, R.A. (2001). Energetic proton generation in ultra-intense laser-solid interactions. *Phys. Plasmas* **8**, 542–549.

Zepf, M., Clark, E.L., Krushelnick, K., Beg, F.N., Escoda, C., Dangor, A.E., Santala, M.I.K., Tatarakis, M., Watts, I.F., Norreys, P., Clarke, R.J., Davies, J.R., Sinclair, M.A., Edwards, R.D., Goldsack, T.J. Spencer, I. & Ledingham, K.W.D. (2001). Fast particle generation and transport in laser–solid interactions. *Phys. Plasmas* **8**, 2323–2330.